Optically Detected Magnetic Resonance of Porphyrin Complexes in the Bacterium *Rhodopseudomonas sphaeroides*

J. Beck, J. U. von Schütz, and H. C. Wolf

Physikalisches Institut, Teilinstitut 3, Universität Stuttgart, Pfaffenwaldring 57, D-7000 Stuttgart 80, Bundesrepublik Deutschland

Z. Naturforsch. **38 c**, 220–229 (1983); received January 10, 1983

Biosynthesis, Bacteriochlorophyll, *Rhodopseudomonas sphaeroides*, Fluorescence

By ODMR in zero-field the porphyrins of the BChl-biosynthesis in whole cells of *Rhodopseudomonas sphaeroides* R-26 are investigated. In the optical emission spectrum 11 pigments could be identified using ODMR in combination with emission and excitation spectroscopy. The properties of these pigments were analyzed in respect to their interactions with the surrounding molecules. An energy transfer from the triplet state of Zn-protoporphyrin to the antenna pigment singlet system was proved by DE-ODMR. The wavelength dependence of the zfs parameters within the individual emission band is explained by a model of selective spin-orbit-coupling. In the case of the precursors chlorophyllide *a* and pheophorbide *a*, for example, we could show that the pigments are bound to proteins via a hydrogen bond to the ketocarbonylgroup of ring V and that porphyrins with a central Mg-atom have an additional bond via a fifth ligand of the Mg.

Introduction

The total spectrum of the optical emission of the photosynthetic bacteria *Rhodopseudomonas (Rps.) sphaeroides* "wild type" and the carotinoidless mutant "R26" was first analyzed by Kaiser [1–3] with the method of fluorescence excitation spectroscopy and by Beck [4–6] with optically detected magnetic resonance in zero-field (ODMR) using the correlation between the optical emission- and excitation spectra as well as the zero-field splitting (zfs) parameters of the triplet state for the identification of the emitting molecules.

It could be demonstrated that in whole cells the emission of the BChl-protein complexes of the photosynthetic apparatus represents only a very restricted region of the total emission spectrum and that the emission in the region of 580–850 nm belongs to many different porphyrin complexes which are BChl-precursors, produced by the biosynthesis of BChl in the photosynthetic bacteria. Because of the broad and overlapping emission- and excitation spectra it was only possible to identify a few of the emitting molecules by means of optical spectroscopy.

In the present paper we used the triplet state of these porphyrins as an additional internal probe which is very sensitive to inter- and intra-molecular interactions and to the complexation of the pigments. Using ODMR in combination with selective excitation we could examine the emission bands which are due to the BChl precursors in more detail. Experiments on the fluorescence of the photosynthetic apparatus are reported elsewhere [7, 8].

There were two aims of our work: first to identify the different porphyrins which are known to be produced by the BChl biosynthesis and secondly to use the zfs parameters as a measure for the association of the molecules.

We take advantage of the knowledge that most of the BChl precursors are associated with proteins [9] and therefore, the different porphyrins represent a large number of model systems different in their porphyrin skeleton. So one can study the interactions between the pigments and the proteins to which they are bound.

0341-0382/83/0300-0220 $ 01.30/0

Materials and Methods

Rps. sphaeroides R-26 was grown anaerobically in the medium after Gloe [10]. The cells were centrifugated and redissolved in phosphate buffer twice under nitrogen atmosphere. Subsequently they were centrifugated again and redissolved in phosphate buffer with 10 mM morpholinopropane sulfonic acid (pH 7). After two-fold dilution with extremely pure glycerol (1 cm cuvette) the samples were diluted to an optical density of 1 at 590 nm and quickly frozen to liquid helium temperature.

Zero field resonance was detected via the technique of fluorescence detected microwave resonance (F-ODMR) [11] and delayed emission detected microwave resonance (DE-ODMR) [12]. F-ODMR as well as DE-ODMR means that the microwave is swept at fixed optical wavelengths. In contrast to these experiments E-MDR means that the optical wavelength is scanned over the total emission spectrum at fixed microwave frequency the power of which is amplitude modulated [13, 14].

Broadband excitation (400–450 nm) was performed using a XBO 450 light source followed by H_2O-, $CuSO_4$-, KV 399-(Schott), DT 450- and DT 470 (Balzers)-filters. For selective excitation of the different porphyrins we used a Laser system consisting of an Argon laser (Spectra Physics Mod. 164-07) and a cw-dye laser (Spectra Physics Mod. 375) with rhodamine 6G and rhodamine 101. The emission was monitored with a 0.6 m Jobin Yvon model HRS 1 grating monochromator fitted with a cooled photomultiplier (extended S 20). The microwave sources were HP models 8690 B and 8620 A followed by Hughes model 1177 TWT power amplifiers and a LWA 110-4.

A digital multipulse time base synchronized the repetitive sweeps with the sweep of the CAT. The E-MDR spectra were recorded by AM-modulation of the microwave power and a lock-in analyser (Ithaco dynatrac 3).

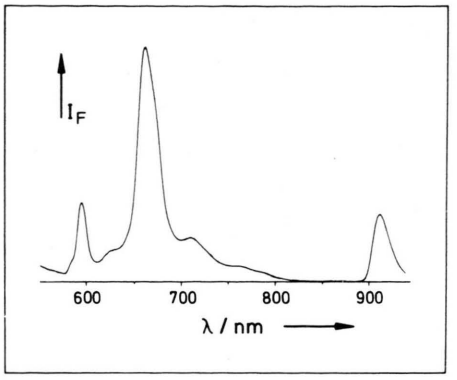

Fig. 1. Total emission of whole cells from *Rps. sphaeroides* R-26 at $T = 1.7$ K. The emission of the BChl precursors appears in the spectral region from 580–850 nm, the fluorescence of the antenna system occurs between 859 and 950 nm.

Results

F-ODMR

Fig. 1 shows the total emission of *Rps. sphaeroides* R-26. The spectral region from 850–950 nm is attributed to the fluorescence of the antenna complexes which will not be discussed here. F-ODMR experiments were performed within the emission from 580 to 850 nm which belongs to the porphyrin-complexes of the BChl biosynthesis. The F-ODMR signals occur in general at frequencies between 200 and 1400 MHz, depending in amplitudes and transition frequencies strongly on the wavelength of detection.

This is demonstrated in Fig. 2 for the spectral region between 580 and 600 nm. We always obtain two signals, *e.g.* the lowest row of Fig. 2 shows broad $|D|-|E|$- and $|D|+|E|$-signals detected at 582 nm which have their maxima at 875 and 1237 MHz. They were attributed to a molecule called pigment I.

Changing the wavelength of detection stepwise from 582 nm to 596 nm the ODMR maxima are shifted slightly and the two positive signals are superimposed by two negative signals, different in frequency and linewidth. At 600 nm the transitions of pigment I have disappeared and only the negative signals with maxima at 768 and 1246 MHz can be seen. They are attributed to a molecule called pigment II.

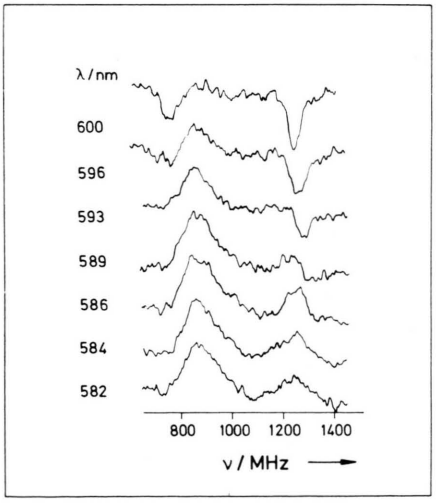

Fig. 2. F-ODMR signals, as detected via the fluorescence of whole cells from *Rps. sphaeroides* R-26 in the wavelength range from 582–600 nm with broad band excitation (400–450 nm).

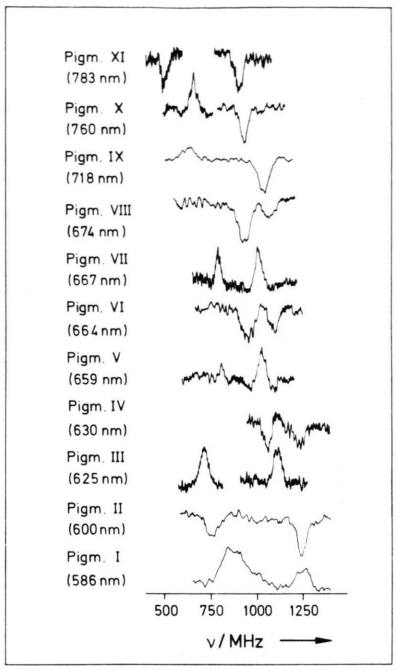

Fig. 3. Summary of the F-ODMR signals detected on the fluorescence of whole cells from *Rps. sphaeroides* between 580 and 850 nm. Different signals are attributed arbitrarily to pigments I–XI. The signals are measured at the wavelength of maximum ODMR-signal-amplitude which is given in brackets. All signals are normalized to the same height.

In the same way the F-ODMR signals of all pigments emitting between 580 and 850 nm were measured. All results are represented in Fig. 3. The triplet states are attributed to pigments I–XI and the wavelength of the maximum signal amplitude is given in brackets.

The optical excitation of the sample was a further parameter of the experiment to obtain additional resolution. It was performed in several ways using the excitation data from Kaiser [1–3]. The signals of the pigments I, II and IV *e.g.* were measured with broad band excitation, whereas the other pigments were excited selectively with respect to their excitation bands.

Table I summarizes the transition frequencies, the zfs-parameters, the wavelengths of detection and the wavelengths of excitation from the pigments I–XI.

DE-ODMR

The spectrum of the delayed emission with maxima at 713, 790 and 913 nm as known from [1–3] is shown in Fig. 4. The DE-ODMR transitions detected at different wavelengths occur between 750 and 1400 MHz (Fig. 5). Table II summar-

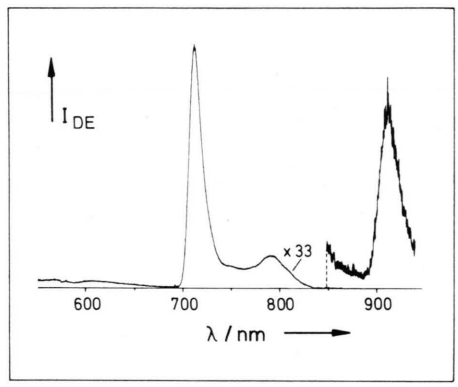

Fig. 4. Spectrum of the delayed emission from whole cells of *Rps. sphaeroides* R-26 at 1.7 K.

Table I. Summary of the fluorescence wavelengths, the ODMR-transition frequencies, the zfs-parameters and the excitation wavelengths from the signals attributed to the pigments I–XI according to Fig. 3.

	Fluor. [nm]	$\lvert D\rvert + \lvert E\rvert$ [MHz]	$\lvert D\rvert - \lvert E\rvert$ [MHz]	$2\lvert E\rvert$ [MHz]	$\lvert D\rvert$ [10^{-4} cm^{-1}]	$\lvert E\rvert$ [10^{-4} cm^{-1}]	Excitation [nm]
Pigm. I	584	1256	872	381	351	63	400–450
Pigm. II	600	1246	768	476	332.2	70.9	400–450
Pigm. III	630	1104	706	395	298.7	65.8	454
Pigm. IV	630	1230	1056	–	377.2	28.8	400–450
Pigm. V	659	1036	810	–	304.7	37.3	624
Pigm. VI	661	1089	949	–	336.2	23.1	501.7
Pigm. VII	667	1007	788	–	296.1	36.2	610
Pigm. VIII	674	1066	934	–	329.9	21.8	514
Pigm. IX	718	1038	642	397	277.2	65.3	514
Pigm. X	760	932	655	285	261.9	45.6	530
Pigm. XI	783	901	490	–	229.5	67.9	590

Table II. Listing of the DE-ODMR transition frequencies detected at different wavelengths on the delayed emission and the calculated zfs-parameters.

Delayed emission [nm]	$\|D\| - \|E\|$ [MHz]	$\|D\| + \|E\|$ [MHz]	$2\|E\|$ [MHz]	$\|D\|$ [10^{-4} cm^{-1}]	$\|E\|$ [10^{-4} cm^{-1}]	Excitation [nm]
700	980	1142	–	350	27	390–480
713	975	1194	229	358	36	390–480
725	908	1223	–	351	52	390–480
740	916	1237	–	355	53	390–480
780	940	1233	–	359	48	390–480
795	919	1250	–	357	54	390–480
911	861	1256	–	350	65	390–480

Error bars ± 30 MHz. D, E ± 5×10^{-4} cm^{-1}.

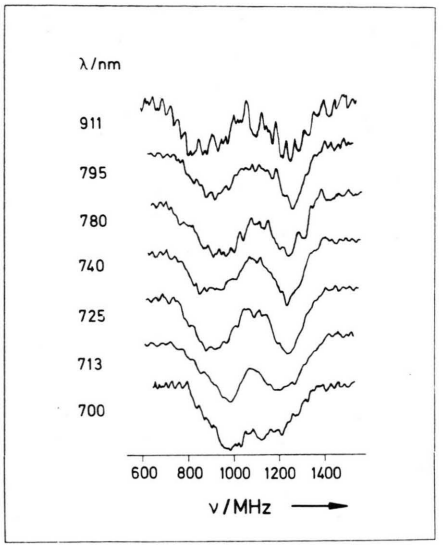

Fig. 5. DE-ODMR signals of whole cells from *Rps. sphaeroides* R-26 at different wavelengths of detection at $T = 1.7$ K. The signals are normalized to the same height.

izes the transition frequencies, the zfs parameters and the wavelengths of detection from Fig. 5.

E-MDR-spectra

In contrast to the F-ODMR and DE-ODMR spectra in which the microwave frequency is scanned continuously at fixed optical wavelength, in E-MDR experiments the microwave-frequency is fixed but amplitude-modulated in a way that only the transitions in the triplet state of one molecule are induced. Doing this, only the emission of this molecule is modulated and selected by scanning the optical spectrum when the emission is detected with a lock-in. In addition phase sensitive detection allows to separate positive and negative ODMR signals.

This is demonstrated by the E-MDR spectrum of pigment I + II in Fig. 6. The positive maxima at 587 and 645 nm belong to pigment I having positive ODMR signals (see Fig. 2) and the negative maxima at 601 and 658 nm to pigment II with negative ODMR signals. As it will be shown in the discussion the negative maxima at 713 and 790 nm result from the delayed emission (see Fig. 5) which can be identified in this spectral region as the phosphorescence of pigment I.

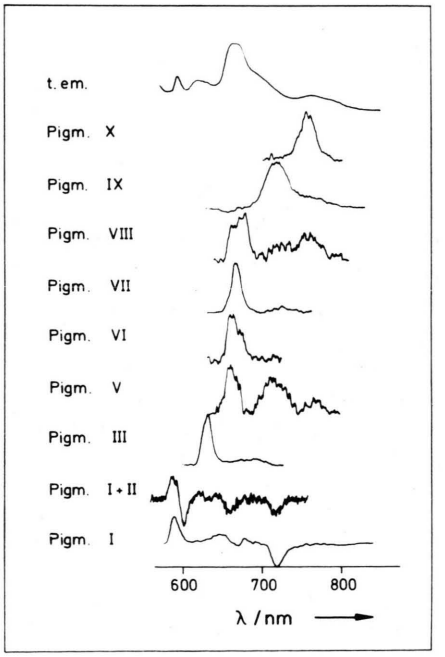

Fig. 6. Comparison of the E-MDR spectra of the BChl precursors (pigment I–XI) with the spectrum of the total emission (t. em.) of whole cells from *Rps. sphaeroides* R-26. The spectra are normalized to the same height. Because of the weak F-ODMR signals of the pigments IV and XI it was not possible to measure E-MDR spectra).

Table III. Summary of the maxima of the E-MDR spectra from the pigments I–X in Fig. 6, and the excitation wavelengths, the RF frequencies as well as the AM-modulation frequencies which were used for the E-MDR experiments.

	Max. of the E-MDR spectra [nm]	Excitation [nm]	RF-frequency [MHz]	AM-frequency [Hz]
Pigm. I	**587**, 645, **713**, 790	400–450	1000–1020	2.8
Pigm. II	**601**, 658	400–450	1250–1270	2.8
Pigm. III	**629**, 685	454	1060–1130	2.8
Pigm. V	**659**, 717, 770	624	1000–1030	10.4
Pigm. VI	**663**, 674	501.7	930–970	10.4
Pigm. VII	**667**, 725	610	995–1027	10.4
Pigm. VIII	664, **674**, 723, 755	514	905–955	10.4
Pigm. IX	**718**, 771	514	1020–1055	10.4
Pigm. X	**757**	530	620–670	10.4

Table IV. Halfwidths of the $|D|+|E|$ and $|D|-|E|$ signals and the shifts of these transitions (in MHz) within the emission band (in cm^{-1}) of the pigment to which they are belonging to.

	ODMR-halfwidths		Shift parameters	
	$\|D\|+\|E\|$ [MHz]	$\|D\|-\|E\|$ [MHz]	$\|D\|+\|E\|$ [MHz/cm^{-1}]	$\|D\|-\|E\|$ [MHz/cm^{-1}]
Pigm. I	131	136		
Pigm. II	49	46		
Pigm. III	39	61	0.09	0.04
Pigm. IV	55	45		
Pigm. V	41	38	0.12	0.05
Pigm. VI	48	50		
Pigm. VII	38	28	0.06	0.07
Pigm. VIII	56	61	0.07	0.04
Pigm. IX	62	76	0.04	
Pigm. X	40	27		
Pigm. XI	46	28		
DE-ODMR	140	140		

Further, in Fig. 6 the total emission spectrum (t. em.) is compared with the E-MDR spectra of the different pigments which have been detected by F-ODMR (Fig. 3). The selectivity of the E-MDR is altered by a well defined excitation of the different pigments as it was done in the F-ODMR experiments. The maxima of the spectra, the excitation wavelength, the RF- and the AM-modulation frequencies are summarized in Table III.

Wavelength dependence of the zfs-parameters

All ODMR transitions are inhomogeneously broadened and dependent on the wavelength of detection within the emission band of *one* molecule. As an example, this is demonstrated at pigment III. In Fig. 7 one can clearly see that the maxima of the ODMR signals shift to lower frequencies with increasing wavelength: The $|D|+|E|$ transition changes with 0.091 MHz/cm^{-1} and the $|D|-|E|$ transition with 0.042 MHz/cm^{-1}. The other pigments show shifts in the same magnitude. As far as they could be determined they are listed in Table IV where the inhomogeneous linewidths of the ODMR transitions are given additionally.

Discussion

Identification of the pigments

The identification of the pigments I–XI was performed on the basis of the zfs-parameters and the E-MDR-spectra in combination with the results of the excitation spectroscopy [1–3]. At first the zfs-parameters were compared with those of different porphyrins and metalloporphyrins "*in vitro*". As it was demonstrated by Kleibeuker [15, 16] there is a distinct correlation between the wavelength of emis-

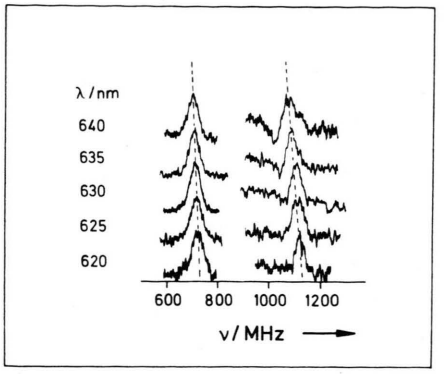

Fig. 7. |D| + |E|- and |D| − |E| transitions of pigment III dependent of the wavelength of detection *within* the fluorescence band of pigment III. The signals are normalized to the same height.

sion and the zfs-parameter D. This can be seen in Fig. 8 in the case of the molecules 1−9 in non-hydrogen-bonding solvents [15, 16].

Using this correlation in order to decide whether there is a porphyrin with or without a central metal ion the fluorescence wavelengths and the values of D from the pigment I−XI were also represented in Fig. 8.

Furthermore this correlation allowed a rough classification of the chemical structure of the porphyrin skeleton. It is obvious *e.g.* that pigment XI has a bacteriochlorin structure.

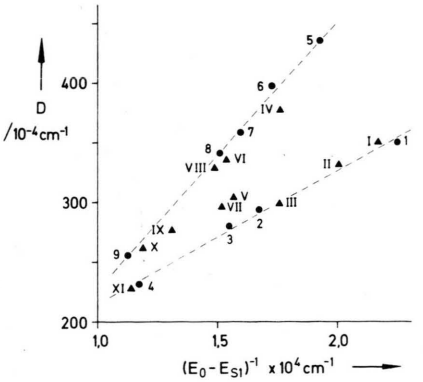

Fig. 8. Correlation between the energy level of S_1 (maximum of the fluorescence) and the zfs-parameter D for different porphyrins and metallo-porphyrins (●) in non-hydrogen-bonding solvents as given in the literature [15, 16] according to the theoretical calculations in [6, 15] (1 = Mg-Porphin, 2 = Chl b, 3 = Chl *a*, 4 = BChl *a*, 5 = Porphin, 6 = Dihydroporphin, 7 Ph *b*, 8 = Ph *a*, 9 = BPh *a*). For comparison the data from the pigments I−XI (▲) are plotted additionally.

The second step of identification was a comparison of the E-MDR spectra with data from "*in vitro*" porphyrins to select between identical porphyrin rings and different side groups with the assumption that there are only "natural" porphyrins present in the membranes of whole cells.

The third and last step is a detailed analysis of the zfs-parameters *and* the emission spectra taking into account the values of porphyrins "*in vitro*" with similar chemical structure.

The results for the pigments I−XI detected on the *prompt fluorescence* are listed in Table V together with the zfs parameters and the wavelengths of their fluorescence maxima.

The identification of the pigments which are the origins for the *delayed emission* is more complicated.

The maxima of the delayed emission at 713 and 790 nm and their excitation spectra, which are identical with that from pigment I, are fingerprints for phosphorescence of Zn-protoporphyrin IX (pigment I). This is confirmed by the DE-ODMR signals, which occur in the same frequency range and which have the same linewidth as those from pigment I but are negative in sign.

According to the explanation of the optical detection of magnetic resonance via the fluorescence or the phosphorescence by van Dorp [11] a decrease in phosphorescence (negative DE-ODMR signal) (resulting from a decrease in the triplet state population) leads to an increase of the singlet ground state population and consequently to an increase in the fluorescence intensity (positive F-ODMR signal) [6, 17]. Therefore, the sign reversal observed in the ODMR by changing from the detection of the fluorescence to the delayed emission is consistent with the picture of a phosphorescent emission of Zn protoporphyrin IX (pigment I) between 690 and 830 nm.

The very weak band at 913 nm could not be associated with a phosphorescence of pigment I although the excitation spectra [1−3], the frequencies of the DE-ODMR signals and their signs are identical. The phosphorescence spectrum of Zn-protoporphyrin IX "*in vitro*" [1−3] doesn't exhibit any band in this region.

Therefore we explain the delayed emission at 913 nm with the fluorescence of the *antenna system* which is pumped by the phosphorescence of pigment I. In this case the excitation spectra are the same and it is also reasonable that the ODMR

Table V. Summary of the pigments identified by our experiments and the corresponding zfs-parameters and fluorescence maxima.

Pigment	$\|D\|$ [10^{-4} cm^{-1}]	$\|E\|$ [10^{-4} cm^{-1}]	Maxima of emission [nm]	Identified as
Pigm. I	351	63.4	**587**, 645, 713[a], 790[a]	Zn-protoporphyrin IX
Pigm. II	332.2	70.9	**601**, 658	Mg-protoporphyrin IX
Pigm. III	298.7	65.8	**629**, 685	Mg-2,4-divinylphaeoporphyrin-a_5-monomethylester
Pigm. IV	377.2	28.8	**630**	protoporphyrin IX
Pigm. V	304.7	37.3	**658**, 717	Mg-2-devinyl-2-hydroxyethyl-chlorophyllid *a*
Pigm. VI	336.2	23.1	**662**, 675	2-devinyl-2-hydroxyethyl-pheophorbid *a*
Pigm. VII	296.1	36.2	**667**, 725	chlorophyllid *a*
Pigm. VIII	329.9	21.8	**675**, 723	pheophorbid *a*
Pigm. IX	277.2	65.3	**718**, 771	2-desacetyl-2 α-hydroxyethyl-bacteriopheophorbid *a*
Pigm. X	261.9	45.6	**757**, 723	bakteriopheophorbid *a* (bakteriopheophytin)
Pigm. XI	229.5	67.9	**783**	bakteriochlorophyllid *a* (bakteriochlorophyll)

[a] Phosphorescence.

signals of the triplet state from which the antenna system is populated are detected at 913 nm with the same sign, because the decrease in the triplet concentration results also in a decrease of the emission of the antenna which is pumped by triplet-singlet energy transfer [6, 18, 19].

In conclusion the delayed emission is a superposition of two spectra: the phosphorescence of Zn protoporphyrin IX (pigment I) in the spectral region from 690–830 nm and the fluorescence of the antenna system with a maximum at 913 nm being pumped by this phosphorescence.

Comparing the molecules identified by our spectroscopic methods in whole cells of *Rps. sphaeroides* R-26 with those which are predicted for the biosynthesis of BChl from other experiments [9] (Fig. 9) it can be seen that with the exception of 2-desacetyl-2-α-hydroxyethylbacteriochlorphyllide all porphyrinstructures of Fig. 9 with and without a central Mg-atom are present in the "*in vivo*" state.

The F-ODMR, DE-ODMR and E-MDR experiments are in general a powerful analytical disentangling method for complex spectra, which consist of a superposition of the emissions from different molecules.

Wavelength dependence

A correlation between the ODMR-transition frequencies and the wavelength of detection within an inhomogeneous broadened emission band is already known for biological molecules in frozen glasses [20, 21], where ODMR was detected *via* the phosphorescence. This correlation with detection *via* the fluorescence was observed for the first time in porphyrins "*in vitro*" by Avarmaa [16, 22] and for porphyrins "*in vivo*" [4, 5].

The broad inhomogeneous lines are thought to be due to a multiplicity of "sites" with different "crystal fields". A theoretical explanation for the correlation between the shift in the fluorescence by the crystal field and the zfs-parameters is given by Lemaistre and Zewail [23, 24]. Following the ideas of Harris [25] they assumed a selective spin-orbit coupling. Within the framework of this theory a linear correlation of the shift in fluorescence and that in the ODMR transitions is predicted. Our experiments do confirm this linear relation (see Fig. 7). The shifts are summarized in Table IV being in excellent agreement with those given in the literature [20–24]. Avarmaa for example measured 0.09 MHz/cm^{-1} in the case of protochlorophyll in *n*-octane.

In conclusion the model of selective spin-orbit-coupling gives a plausible explanation for the effect of different crystal fields on the ODMR transitions in pigment-protein-complexes.

Protein binding of the BChl-precursors

The BChl-precursors occurring in the biosynthetic pathway are assumed to be active in biosynthesis

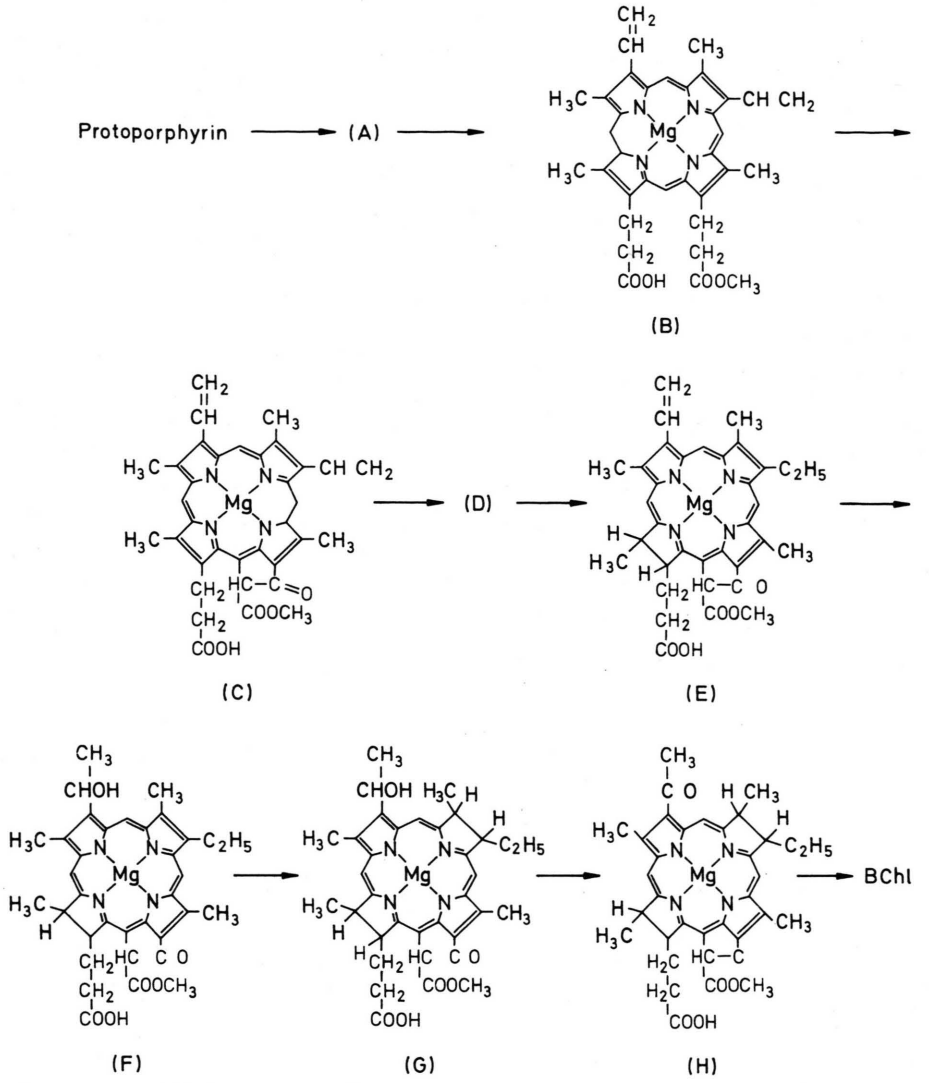

Fig. 9. Proposed biosynthetic route from protoporphyrin to BChl *a* according to Jones [9]. (A) means Mg-protoporphyrin, (B) = Mg-protoporphyrin monomethyl ester, (C) = Mg-2, 4-divinyl pheoporphyrin a_5 monomethyl ester, (D) = Mg-2-vinyl, 4-ethyl pheoporphyrin a_5 monomethyl ester, (E) = Chlorophyllide *a*, (F) = 2-Devinyl, 2-hydroxyethyl chlorophyllide *a*, (G) = 2-Desacetyl-2-hydroxyethyl bacteriochlorophyllide *a* and (H) = Bacteriochlorophyllide *a*.

only when they are complexed with special proteins [9]. This is proved by the macromolecular complexes which are excreted by different mutants in different stages of the biosynthesis. For example Mg-2,4-divinylphaeporphyrin a_5 monomethylester is excreted as a complex with 49% of protein, 44% of lipids and 7% of pigment.

Furtheron fluorescence excitation experiments on membrane fractions of Reidl [26] showed that the BChl-precursors are located in the membranes. From this it can be concluded that at least the pigments III, V and XI are bound in the cytoplasma-membrane within pigment-protein-lipid complexes.

We now use the precursor-complexes as model systems for analyzing the bindings between the porphyrin and the protein and we discuss the conclusions which can be made from the results of our ODMR measurements.

The porphyrin-molecule has two main possibilities for a binding to molecules in the environment

[15]. The first is the formation of one or two further ligands by the Mg-atom and the second is a hydrogen-bonding of the carbonyl groups which are attached to the porphyrin ring. Interactions of the lipids in the complexes with the phytol tail of the porphyrins are not possible because the phytylisation is the last step in biosynthesis [9].

For separating these two binding possibilities we have to compare the ODMR-data of a Mg-porphyrin-precursor and the Mg-free pigment belonging to it. For example we analyze chlorophyllide *a* (pigment VII) and pheophorbide *a* because we have a large number of ODMR data from different solvent complexes of these molecules "*in vitro*".

For investigating hydrogen bonds to the carbonyl groups we regard pheophorbide *a* (pigment VIII) which has the identical porphyrin ring as pheophytin *a* but has no phytol tail. This Mg-free porphyrin has 3 carbonylgroups but only the ketocarbonylgroup of ring V is interacting with the electron-system and in consequence only hydrogen bonding to this group has an influence on the ODMR transitions.

Comparing now the zfs-parameters of pheophorbide *a* (Table VI) with pheophytin *a* as a solvent complex it is important to know that only with ethanol as a solvent hydrogen bonds to the ketocarbonyl-group are formed and not with MTHF and *n*-octane. In Table VI it can be seen unambiguously from the value of D that in the pheophorbide *a*-protein-complex the porphyrin must be bound to the protein by a hydrogen bond with the ketocarbonyl-group of ring V.

Turning to the comparison of the zfs-parameter of chlorophyllide *a* with those of Chl *a* × H_2O complexes "*in vitro*", it is remarkable in Table VII that D is consistent with a monoligated complex. This is in accordance with resonance Raman and X-ray structure measurements on BChl-protein complexes [27–30] which show that the central Mg-atom is interacting via a fifth ligand with a hystidine group of the protein.

Table VI. Comparison of the zfs-parameters and the fluorescence maxima of pigment VIII (pheophorbide *a*) and pheophytins in different solvent complexes.

Pigment	D [10^{-4} cm^{-1}]	E [10^{-4} cm^{-1}]	Maxima of fluorescence [nm]	Matrix	Ref.
Pigment VIII	329.9	21.1	**674**	whole cells *Rps. sphaeroides* R-26	this work
Pheophytin *a*	350	20	**675**	*n*-octane	16
Pheophytin *a*	341	33	**667.5**	MTHF	16
Pheo *a* × eth.	334	26		ethanol	15

Table VII. Comparison of the zfs-parameters and fluorescence maxima of pigment VII (chlorophyllide *a*) with different Chl *a*-solvent complexes and pyrochlorophyllide *a* protein complexes.

	|D| [10^{-4} cm^{-1}]	|E| [10^{-4} cm^{-1}]	Maxima of fluorescence [nm]	Matrix	Ref.
Pigment VII	296.1	36.2	**667**, 725	whole cells *Rps. sphaeroides* R-26	this work
Chl *a* × H_2O	296	43.9	**670**	*n*-octane	31
Chl *a* × 2 H_2O	274	34.3	**680**	*n*-octane	31
Chl *a* × 2 Pyr	283 ± 5	40 ± 5	**686**	*n*-octane + pyridin	16, 33
Pyro-chlorophyllid *a*	296	37.6	**668**	protein-complex	32
Pyro-chlorophyllid *a*	294	36.6	**671**	protein-complex	32
Pyro-chlorophyllid *a*	280	32.5	**685**	protein-complex	32

Furtheron the fluorescence and the zfs parameters of a pyrochlorophyllide *a*-protein-complex measured by Clarke [31, 32] are nearly identical (Table VII) with our values and give an additional confirmation of our results.

In conclusion our F-ODMR experiments show that the binding of the porphyrin to the protein occurs via a hydrogen-bond to the ketocarbonylgroup and in case of Mg-porphyrins an additional bond via the fifth ligand of the central Mg to a hystidine group of the protein must be present.

With this interpretation it is not necessary to explain the decay rates of the pyrochlorophyllide-complex reported by Clarke [27, 28] with a sixth ligand formed by the Mg-atom. The observed increase of the decay rates relative to the monoligated Chl $a \times H_2O$ complex can be also explained by a hydrogen bond to the ketocarbonylgroup [10] which results from our experiments.

Acknowledgements

We thank Prof. T. J. Schaafsma and Prof. H. Scheer for valuable discussions. This work was supported by the Deutsche Forschungsgemeinschaft.

[1] G. H. Kaiser, Dissertation, Universität Stuttgart (1980).
[2] G. H. Kaiser, J. Beck, J. U. von Schütz, and H. C. Wolf, Biochim. Biophys. Acta **634,** 153 (1981).
[3] G. H. Kaiser, J. Beck, J. U. von Schütz, and H. C. Wolf, in Photosynthesis, Proceedings of the 5th Int. Photosynthesis Congr., Halkidiki, Greece, (G. Akoyunoglou, ed.), **Vol. I,** p. 69, Balaban, International Science Services, Philadelphia 1981.
[4] J. Beck, G. H. Kaiser, J. U. von Schütz, and H. C. Wolf, Biochim. Biophys. Acta **634,** 165 (1981).
[5] J. Beck, J. U. von Schütz, and H. C. Wolf, in Photosynthesis, Proceedings of the 5th Int. Photosynthesis Congr., Halkidiki, Greece, (G. Akoyunoglou, ed.), **Vol. I,** p. 89, Balaban, International Science Services, Philadelphia 1981.
[6] J. Beck, Dissertation, Universität Stuttgart 1982.
[7] J. Beck, J. U. von Schütz, and H. C. Wolf, Chem. Phys. Letters **94,** 141 (1983).
[8] J. Beck, J. U. von Schütz, and H. C. Wolf, Chem. Phys. Letters **94,** 147 (1983).
[9] O. T. G. Jones, in The Photosynthetic Bacteria (R. K. Clayton and W. R. Sistrom, eds.), p. 369, Plenum Press, New York 1978.
[10] A. Gloe, N. Pfennig, H. Brockmann, and W. Trowitzsch, Arch. Microbiol. **102,** 103 (1975).
[11] W. G. van Dorp, T. J. Schaafsma, M. Soma, and J. H. van der Waals, Chem. Phys. Letters **21,** 221 (1973).
[12] W. Steudle, Dissertation, Universität Stuttgart 1979.
[13] M. A. El Sayed, MTP Int. Rev. Sci. Phys. Chem.: Ser. one, **Vol. 3,** p. 119, Butterworths, London 1972.
[14] S. J. van der Bent, Dissertation, Landbouwhogeschool Wageningen 1977.
[15] J. F. Kleibeuker, Dissertation, Landbouwhogeschool Wageningen 1977.
[16] T. J. Schaafsma, in Triplet State ODMR Spectroscopy (R. H. Clarke, ed.), Chapter 8, p. 346, John Wiley and Sons, New York 1982.
[17] W. R. Leenstra, M. Gouterman, and A. L. Kwiram, Chem. Phys. Letters **65** (2), 278 (1979).
[18] G. H. van Brakel, Dissertation, Landbouwhogeschool Wageningen 1982.
[19] A. H. Maki and T. Co, Biochemistry **15,** 6, 1229 (1976).
[20] J. U. von Schütz, J. Zuclich, and A. H. Maki, J. Am. Chem. Soc. **96,** 714 (1974).
[21] A. H. Maki and J. A. Zuclich, in Topics in Current Chemistry, **Vol. 54,** p. 116, Springer, Berlin 1975.
[22] R. Avarmaa and T. J. Schaafsma, Chem. Phys. Letters **72,** 339 (1980).
[23] J. P. Lemaistre and A. H. Zewail, Chem. Phys. Letters **68,** 296 (1979).
[24] J. P. Lemaistre and A. H. Zewail, Chem. Phys. Letters **68,** 302 (1979).
[25] A. H. Francis and C. B. Harris, Chem. Phys. Letters **9,** 181 (1971).
[26] H. Reidl, private communication (1982).
[27] M. Lutz, in Photosynthesis, Proceedings of the 5th Int. Photosynthesis Congr., Halkidiki, Greece, (G. Akoyunoglou, ed.) **Vol. III,** p. 461, Balaban International Science Services, Philadelphia 1981.
[28] M. Lutz, A. H. Hoff, and L. Brekamet, Biochim. Biophys. Acta **679,** 331 (1982).
[29] J. M. Olson, in The Photosynthetic Bacteria (R. K. Clayton and W. R. Sistrom, eds.) Chapter 8, p. 161, Plenum Press, New York 1978.
[30] R. E. Fenna and B. W. Matthews, in The Porphyrins (D. Dolphin, ed.), **Vol. VII,** Chapter 11, p. 473, Academic Press, New York 1978.
[31] R. H. Clarke, S. Hotchandani, S. P. Jagannathan, and R. M. Leblanc, Chem. Phys. Letters **89,** 41 (1982).
[32] R. H. Clarke, E. B. Haulon, and S. G. Boxer, Chem. Phys. Letters **89,** 41 (1982).
[33] W. R. Leenstra, M. Gouterman, and A. L. Kwiram, J. Chem. Phys. **68,** 327 (1978).